nature genetics

Seed filling in domesticated maize and rice depends on SWEET-mediated hexose transport

Davide Sosso[1], Dangping Luo[2], Qin-Bao Li[3], Joelle Sasse[1], Jinliang Yang[4], Ghislaine Gendrot[5], Masaharu Suzuki[6], Karen E Koch[6], Donald R McCarty[6], Prem S Chourey[3,6], Peter M Rogowsky[5], Jeffrey Ross-Ibarra[7], Bing Yang[2] & Wolf B Frommer[1]

© 2015 Nature America, Inc. All rights reserved.

Carbohydrate import into seeds directly determines seed size and must have been increased through domestication. However, evidence of the domestication of sugar translocation and the identities of seed-filling transporters have been elusive. Maize *ZmSWEET4c*, as opposed to its sucrose-transporting homologs, mediates transepithelial hexose transport across the basal endosperm transfer layer (BETL), the entry point of nutrients into the seed, and shows signatures indicative of selection during domestication. Mutants of both maize *ZmSWEET4c* and its rice ortholog *OsSWEET4* are defective in seed filling, indicating that a lack of hexose transport at the BETL impairs further transfer of sugars imported from the maternal phloem. In both maize and rice, *SWEET4* was likely recruited during domestication to enhance sugar import into the endosperm.

Cell size and number determine seed size and weight and depend on efficient translocation of soluble sugars into developing seeds[1,2]. Developing seeds must be able to efficiently process nutrients delivered from maternal tissues[3,4]. Early farmers and breeders selected large seeds for high caloric value and sturdier seedlings[5]. It is generally accepted that domestication manipulated regulatory processes, for example, hormone signaling[6]; however, there is little evidence for direct selection on the sugar translocation machinery, except in the case of the promoter of a cell wall invertase gene, *OsGIF1* (*OsCIN2*)[2]. By comparison, maize grains are larger, yet little evidence has emerged for selection acting on loci related to sugar metabolism and transport.

To identify potential targets of domestication among genes that encode sugar metabolism and transport proteins, we searched large-scale expression data for candidates with high expression during seed development[7–9]. Of the 54 genes analyzed, 16 were highly expressed in at least one study (**Supplementary Table 1**). Among these, *ZmSWEET4c* was the only locus showing evidence of selection during domestication in a genomic study comparing populations of maize (*Zea mays* L. ssp. *mays*) with the maize ancestor teosinte (*Zea mays* L. ssp. *parviglumis*)[10]. SWEETs function in sugar allocation in plants, from phloem loading to nectar secretion[11–13], making *ZmSWEET4c* a candidate for a role in seed filling.

A genome scan for loci involved in maize domestication identified *ZmSWEET4c* as one of 24 genes in a selected feature on chromosome 5 (**Supplementary Table 2**)[10]. Further genome-wide analysis indicated that *ZmSWEET4c* has lost more nucleotide diversity during domestication relative to 93% of all genes. To more closely investigate diversity at the *ZmSWEET4c* locus, we resequenced 1.5 kb of the promoter, the first three exons and two introns of the *ZmSWEET4c* locus in a small maize and teosinte panel. The *ZmSWEET4c* promoter region showed a particularly striking loss of diversity (**Fig. 1a**), and both the promoter and the first intron showed stronger allele frequency differentiation than expected from a simple domestication bottleneck model (**Supplementary Fig. 1a** and **Supplementary Table 3**). Differences in these noncoding regions are reflected in the diversity estimated across the locus using SNP data from a large panel of maize and teosinte (**Supplementary Fig. 1b**). Although this information was insufficient to pinpoint causal alterations, a potential candidate is a large (78-bp) deletion in the first intron: a diagnostic SNP 3 bp upstream of the indel was present in 92% of the 500 maize lines but in only 36% of the 14 teosinte lines.

Changes in gene expression are prevalent among domestication-related genes[10,14]. Thus, we compared *ZmSWEET4c* expression profiles in developing maize and teosinte grains (**Fig. 1b**). In maize, *ZmSWEET4c* expression increased by 3.4-fold between 10 and 17 days after pollination (DAP), coincident with massive sugar import into wild-type seeds[15]. In contrast, expression in teosinte was on average 75% lower than in maize at 17 DAP (**Fig. 1c**). We speculate that, as early farmers selected larger seeds, they selected elevated sugar import through the developmentally controlled induction of *ZmSWEET4c* expression, thereby producing grains with larger endosperm. In rice, a larger endosperm correlates with changes in *OsGIF1* expression[2]. Although the diversity patterns identified by comparing maize and teosinte were especially striking in the promoter and

[1]Department of Plant Biology, Carnegie Science, Stanford, California, USA. [2]Department of Genetics, Development and Cell Biology, Iowa State University, Ames, Iowa, USA. [3]US Department of Agriculture, Agricultural Research Service (USDA-ARS), Gainesville, Florida, USA. [4]Department of Plant Sciences, University of California, Davis, Davis, California, USA. [5]Ecole Normale Supérieure de Lyon, Université Lyon 1, Unité Reproduction et Développement des Plantes, Lyon, France. [6]Plant Molecular and Cellular Biology, Agronomy Department, University of Florida, Gainesville, Florida, USA. [7]Department of Plant Sciences, Center for Population Biology and Genome Center, University of California, Davis, Davis, California, USA. Correspondence should be addressed to D.S. (dsosso@carnegiescience.edu).

Received 16 April; accepted 23 September; published online 2 November 2015; doi:10.1038/ng.3422

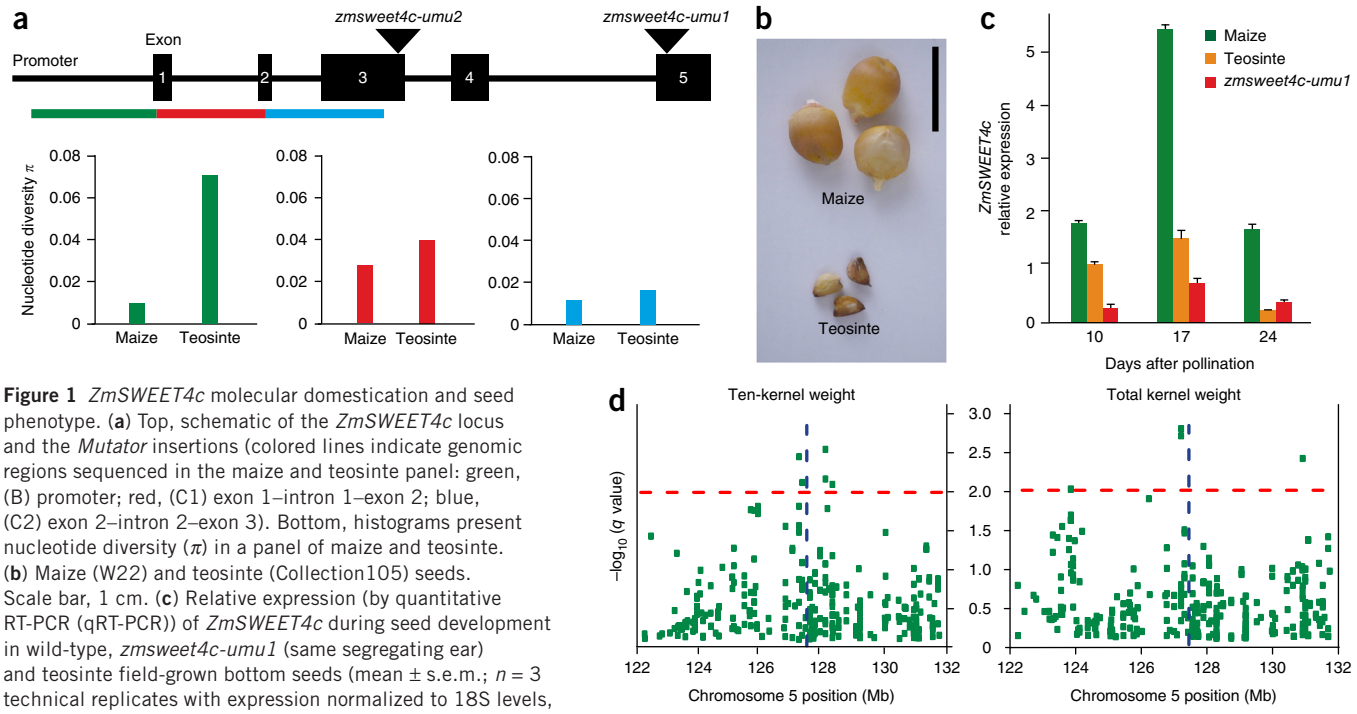

Figure 1 *ZmSWEET4c* molecular domestication and seed phenotype. (**a**) Top, schematic of the *ZmSWEET4c* locus and the *Mutator* insertions (colored lines indicate genomic regions sequenced in the maize and teosinte panel: green, (B) promoter; red, (C1) exon 1–intron 1–exon 2; blue, (C2) exon 2–intron 2–exon 3). Bottom, histograms present nucleotide diversity (π) in a panel of maize and teosinte. (**b**) Maize (W22) and teosinte (Collection105) seeds. Scale bar, 1 cm. (**c**) Relative expression (by quantitative RT-PCR (qRT-PCR)) of *ZmSWEET4c* during seed development in wild-type, *zmsweet4c-umu1* (same segregating ear) and teosinte field-grown bottom seeds (mean ± s.e.m.; $n = 3$ technical replicates with expression normalized to 18S levels, repeated independently three times with comparable results). (**d**) Regional association scan results. Vertical dashed blue lines indicate the center of the *ZmSWEET4c* gene, and horizontal dashed red lines indicate the threshold of FDR = 0.01. The *q* value represents the *P* value for association corrected using the FDR method.

first intron of *ZmSWEET4c*, conclusive analysis of functional differences between maize and teosinte regulatory sequences will require experimental validation, and, currently, neither teosinte nor maize *zmsweet4c* mutant is amenable to transformation.

To test for associations between *ZmSWEET4c* sequences and seed size, we evaluated natural and mutation-induced variation. A candidate gene association analysis using data from a panel of 282 inbred maize lines[16] identified significant (false discovery rate (FDR) < 0.01) associations between SNPs in the promoter region of *ZmSWEET4c* and ten-kernel and total kernel weight after correction for genomic background effects (**Fig. 1d**). These SNPs explained >4% of the total phenotypic variation for both traits and as much as 11% of their heritability. Notably, *zmsweet4c* insertion mutants showed grain defects, including a dramatic loss of endosperm. The *zmsweet4c-umu1* mutant results from a *Mutator* transposon insertion in the last exon of *ZmSWEET4c* (**Fig. 1a**) and behaves as a monogenic recessive trait classified as *empty pericarp* (*emp*)[17] (**Fig. 2a**). The *emp* phenotype, apparent at ~8 DAP, manifested as collapsed grains at ~15 DAP and beyond (**Fig. 2b**). Similar observations were made for the *zmsweet4c-umu2* mutant, which carries a *Mutator* insertion in exon 3 of *ZmSWEET4c* (**Supplementary Fig. 2**). Mature *zmsweet4c-umu1* grains contained ~10-fold less starch and weighed ~9-fold less than wild-type (W22) grains (**Supplementary Fig. 3**). *ZmSWEET4c* transcript abundance was greatly reduced in mutant seeds (**Fig. 1c**). The *zmsweet4c-umu1* mutation also affected embryo size but much less dramatically than the size of the endosperm, compatible with the presence of an alternative sugar translocation pathway. Homozygous-mutant embryos were able to germinate and develop into normal-appearing, fertile plants, implying that the role of *ZmSWEET4c* is specific to seed filling.

Filial tissues—embryo and endosperm—are symplasmically isolated from the maternal seed coat, thus requiring at least two transport steps for nutrients: one secreting sugars from the maternal layers and the second importing sugars into filial tissues[4,18]. Recent work has identified several SWEETs involved in sucrose efflux[19]. ZmSWEET4c could therefore be responsible for sucrose efflux along the phloem-unloading path, such as release of sucrose at phloem termini or the placentochalaza. There are additional sites at which sugar transport activity may be required. Shannon proposed, on the basis of radiotracer studies, that sucrose is cleaved in the phloem-unloading zone[20]. However, studies using sucrose analogs have demonstrated that sucrose cleavage is not required for import into grains[21]. Shannon's hypothesis is strongly supported by the observation that mutation of *ZmMn1* (*ZmIncw2*), encoding a cell wall invertase, reduces endosperm size[4,22,23]. Therefore, ZmSWEET4c could function in sugar translocation toward the endosperm. Analysis of *in situ* hybridization and RNA sequencing (RNA-seq) data indicated that *ZmSWEET4c* expression was abundant in the BETL in comparison to maternal tissues such as phloem termini or placentochalaza[24] (**Supplementary Fig. 4**). The BETL is a unique cell layer of endosperm characterized by massive amplification of the basal membrane surface (transfer cells), reminiscent of the intestinal epithelial cell barrier in humans. SWEETs localize either to the plasma membrane where they secrete sugars[11–13] or transport sugars in and out of the vacuole[25–28]. ZmSWEET4c may thus have one of three alternative roles: sucrose transfer across the BETL, hexose transfer across the BETL or transient vacuolar storage within the BETL. Subcellular localization of ZmSWEET4c-eGFP fusions to the plasma membrane supports a role in mono- or disaccharide transport into BETL cells (**Supplementary Fig. 5**). The function of ZmSWEET4c could thus be one of two alternative roles: sucrose transfer across the BETL or hexose transfer across the BETL. We tested substrate specificity by coexpressing ZmSWEET4c with sucrose or glucose FRET (Förster resonance energy transfer) sensors in HEK293T cell cultures[12]. ZmSWEET4c did not show detectable sucrose transport activity (**Fig. 2c**) but enabled HEK293T cells to accumulate glucose (**Fig. 2d**). The

© 2015 Nature America, Inc. All rights reserved.

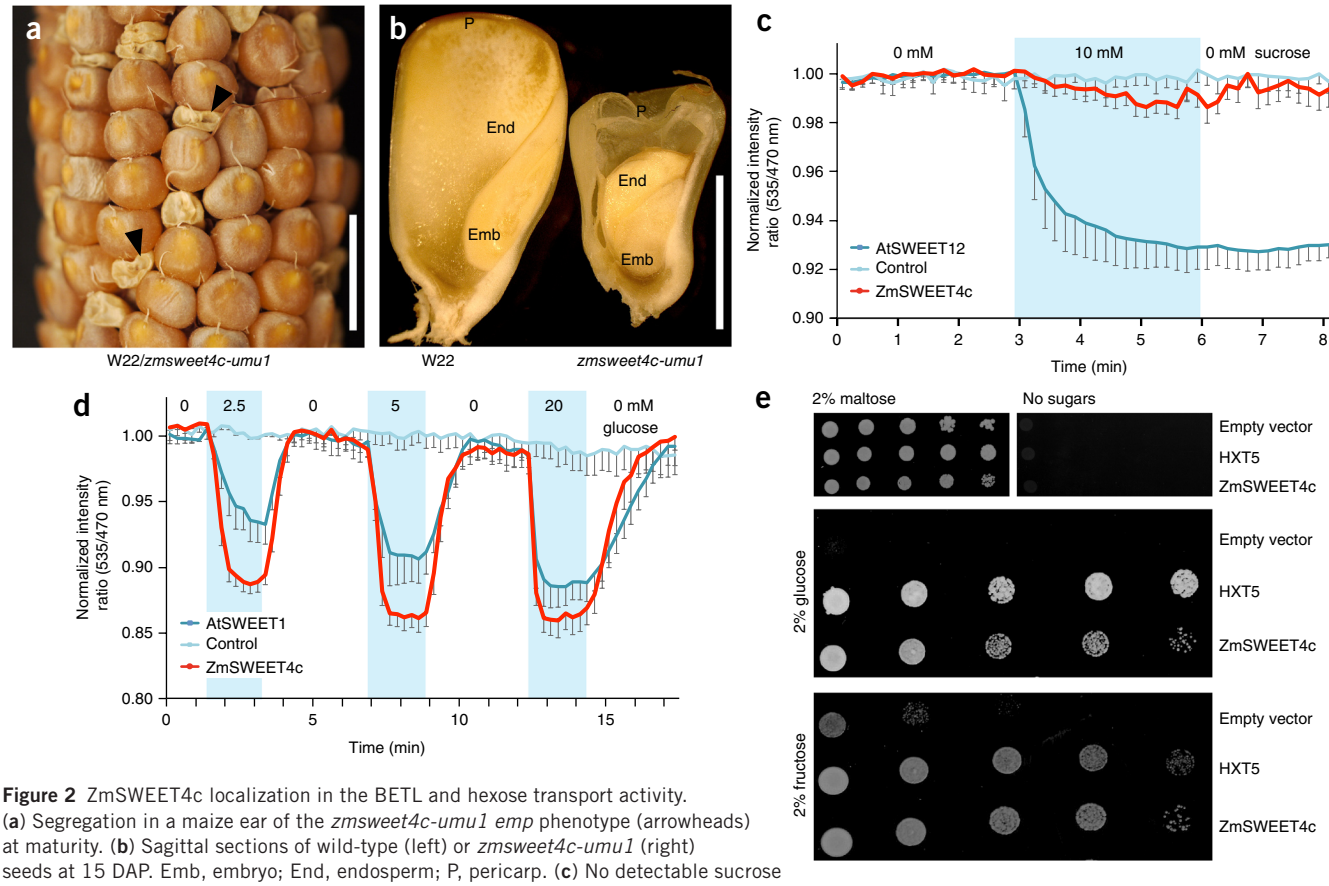

Figure 2 ZmSWEET4c localization in the BETL and hexose transport activity. (**a**) Segregation in a maize ear of the *zmsweet4c-umu1 emp* phenotype (arrowheads) at maturity. (**b**) Sagittal sections of wild-type (left) or *zmsweet4c-umu1* (right) seeds at 15 DAP. Emb, embryo; End, endosperm; P, pericarp. (**c**) No detectable sucrose influx by ZmSWEET4c in HEK293T cells coexpressing the FLIPsuc90μΔ1V sucrose sensor. (**d**) Glucose transport activity by ZmSWEET4c in HEK293T cells coexpressing the FLIPglu600μD13V glucose sensor. Cells were transfected to express sensor only as a negative control or to coexpress AtSWEET1 (glucose) or AtSWEET12 (sucrose) as a positive control. Data are shown as means ± s.e.m., $n \geq 11$ or 13; experiments were repeated with comparable results at least four times. (**e**) Complementation of hexose transport deficiency by ZmSWEET4c in EBY4000 yeast (positive control, yeast HXT5; negative control, empty vector). Scale bars, 1 cm in **a** and 0.5 cm in **b**.

emp phenotype in mutants of the BETL-expressed *ZmMn1* invertase gene[22,23] implicated unknown glucose and fructose transporters in BETL sugar uptake. ZmSWEET4c also complemented the fructose uptake deficiency of the EBY4000 yeast strain[29], indicating efficient fructose transport capability (**Fig. 2e**). Together, our findings intimate that ZmSWEET4c transfers cell wall invertase–derived hexoses into or across the BETL as a key step in seed filling. One may hypothesize that ZmSWEET4c is polarized on the basal BETL membrane and is responsible only for import or, similar to the intestinal glucose uniporter GLUT2 in humans, mediates transepithelial hexose transport[30] (**Supplementary Fig. 6**). Our work places ZmMn1 and ZmSWEET4c into a linear pathway for sugar cleavage, import and export and implies the existence of yet unknown efflux transporters for sucrose at phloem termini and the placentochalaza. Sucrose efflux may potentially be mediated by sucrose-transporting SWEETs, as observed in *Arabidopsis thaliana*[19].

The amplification of cell surface area in the BETL is likely necessary for sustaining high flux rates during seed filling[31,32]. Interestingly, transfer cell characteristics are regulated by sugars, in particular by glucose in legume seeds[33], linking membrane surface area directly to sugar transport and signaling. In maize, we also observed the coincidence of transfer cells, sugar transporters and sugar metabolism. BETL characteristics appear at ~6 DAP (ref. 31). Strikingly, at this stage, *zmsweet4c* (**Fig. 3a** and **Supplementary Fig. 7**) and *zmmn1* mutants failed to develop fully differentiated transfer cells[22]. BETL cell fate is established early during seed development (at ~5 DAP) and involves ZmMRP1 as transcriptional master regulator[34]. *ZmMRP1* expression and, consequentially, BETL cell fate are controlled by sugars[35]. In wild-type, expression of *ZmMn1* and *ZmSWEET4c* preceded that of *ZmMRP1* (**Supplementary Fig. 8**), intimating that ZmSWEET4c-mediated glucose import may induce *ZmMRP1* expression. Consistent with this model, *ZmMRP1* expression was strongly reduced in *zmsweet4c-umu1* seeds, possibly causing the failure to establish the BETL (**Fig. 3b**). *ZmMn1* and *ZmSWEET4c* expression may also be regulated by sugar accumulation in the BETL, as indicated by reduced *ZmMn1* expression in *zmsweet4c-umu1* seeds and by reduced *ZmSWEET4c* expression in *zmmn1* and in wild-type seeds cultured on acarbose-supplemented medium (**Supplementary Fig. 9**). Indeed, *ZmSWEET4c* expression could be induced by glucose during *in vitro* culture of endosperm (**Fig. 3c**). On the basis of these data, we propose two hypotheses for signaling in BETL precursor cells: (i) glucose could induce *ZmMRP1*, *ZmMn1* and *ZmSWEET4c* expression in parallel or (ii) glucose import by basal levels of ZmMn1 and ZmSWEET4c might induce *ZmMRP1* expression to further activate the transfer cell machinery, including induction of *ZmMn1* and *ZmSWEET4c* expression (**Supplementary Fig. 10**). Both hypotheses involve a 'feed-forward' mechanism in which increasing levels of glucose trigger enhanced membrane surface area as well as increased capacity to hydrolyze sucrose and import hexoses into the BETL (**Fig. 3d**). The hypotheses are consistent with data from legumes and cereals, in which glucose triggers transfer cell

© 2015 Nature America, Inc. All rights reserved.

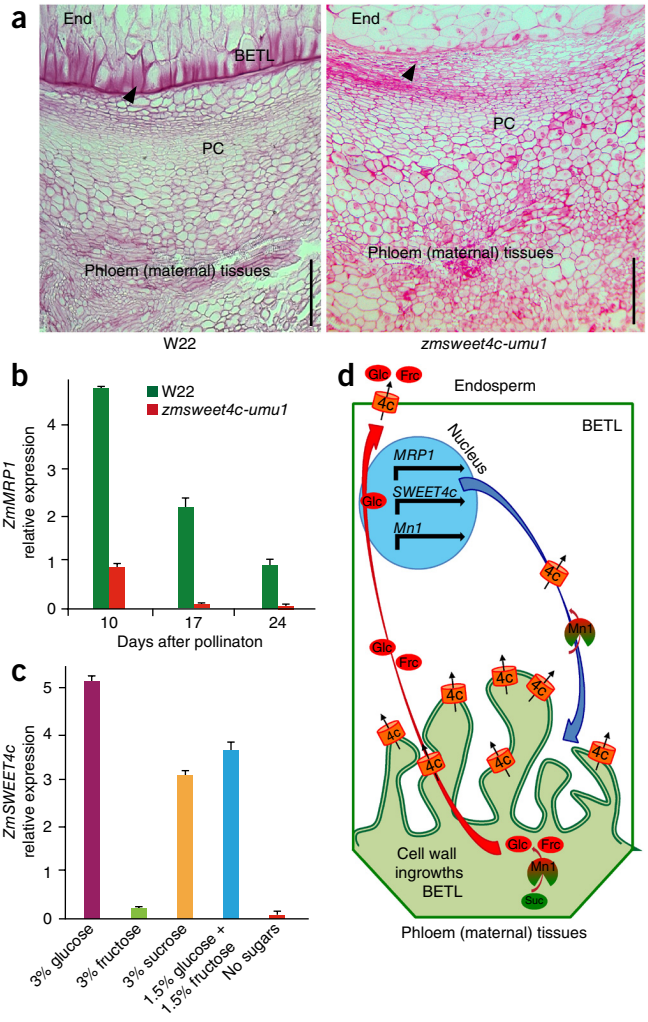

Figure 3 The *zmsweet4c-umu1* mutant has altered BETL development. (**a**) Sagittal sections of seeds at 15 DAP stained with Safranin O showing loss of cell wall invaginations in the *zmsweet4c-umu1* mutant. PC, placentochalaza. Scale bars, 100 µm. (**b**) Relative expression levels of *ZmMRP1* during maize seed development. Expression was measured in wild-type and *zmsweet4c-umu1* bottom seeds. Data are shown as means ± s.e.m., $n = 3$ technical replicates; *ZmMRP1* levels were normalized to 18S rRNA levels. (**c**) Relative expression levels of *ZmSWEET4c* in endosperm cultured *in vitro* on media containing different sugars. Data are shown as means ± s.e.m., $n = 3$ technical replicates; *ZmSWEET4c* levels are normalized to 18S levels. (**d**) Hypothetical model for the feed-forward mechanism of BETL sugar flux. SWEET4c-mediated sugar accumulation in the BETL induces hexose import by increasing membrane area, capacity to hold transporters and V_{max} (maximal velocity) for sugar import as a result of increased ZmSWEET4c total activity. 4c, ZmSWEET4c; Frc, fructose; Glc, glucose; Suc, sucrose.

division and differentiation, whereas at later developmental stages sucrose induces cell expansion and storage[31,36]. In maize, the most parsimonious hypothesis is that sugar supply to the BETL is limited in *zmmn1* and *zmsweet4c* mutants, thereby preventing effective differentiation. At present, *zmmrp1* mutants are not available and the *zmsweet4c-umu1* mutant is difficult to transform, obstructing direct testing of the hypotheses. In contrast to other sugar metabolism–related genes, *ZmMn1* and *ZmMRP1* are more highly expressed in maize than teosinte, indicating that domestication may have preferentially targeted the BETL import machinery, which comprises ZmMn1 and ZmSWEET4c, and increased membrane surface area on the basal side of the BETL (**Supplementary Fig. 11**).

Another way to explore this model is to characterize conservation across species. Maize has three closely related *SWEET4* paralogs, but the striking phenotype of the *zmsweet4c-umu1* mutant and the low expression levels of *ZmSWEET4a* and *ZmSWEET4b* in the grain (**Supplementary Table 1**) suggest a dominant role for ZmSWEET4c in endosperm sugar import. Phylogenetic comparisons[37] showed that *Sorghum bicolor* and *Setaria italica* each have three *SWEET4* genes, whereas *Brachypodium distachyon* has only two (**Supplementary Fig. 12**). Rice (*Oryza sativa*) has only a single homolog, *OsSWEET4*, suggesting that the three paralogs in maize evolved from a single gene in the common ancestor of rice and maize. To test whether *OsSWEET4* serves orthologous functions in rice grain filling, we analyzed its substrate specificity, seed expression and mutant phenotypes. OsSWEET4 functions as a glucose and fructose transporter (**Fig. 4a**), and grain expression of *OsSWEET4* was highest at the base of the spikelet, consistent with that of the *OsGIF1* invertase[2] (**Fig. 4b**). Two independent null mutants created with TALEN (TAL effector nuclease) technology (**Supplementary Fig. 13**) showed a strong *emp* phenotype (**Fig. 4c,d**). Analysis of a promoter-reporter fusion of *OsSWEET4* in rice protoplasts showed that expression of this gene can be induced by glucose (**Supplementary Fig. 14**). As was the case for maize *ZmSWEET4c*, genome scans indicated that the *OsSWEET4* region was also a target of selection during rice domestication[38] (**Supplementary Figs. 15** and **16**).

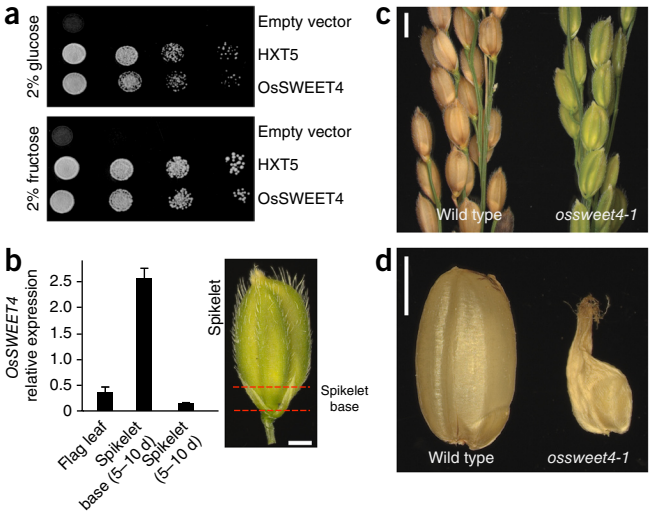

Figure 4 The *ZmSWEET4c* ortholog in *O. sativa* (*OsSWEET4*) is essential for seed filling. (**a**) Complementation of the hexose uptake deficiency of EBY4000 yeast by OsSWEET4. (**b**) *OsSWEET4* expression levels relative to *Actin* (*Os03g50885*) levels in different tissues by quantitative PCR (qPCR). Data are shown as means ± s.e.m., $n = 3$ technical replicates. (**c**,**d**) Visual phenotypes of spikes (**c**) and grains (**d**) for wild-type Kitaake and the TALEN-generated *ossweet4-1* mutant. A mutant involving a second allele shows a comparable phenotype. Scale bars, 1 cm in **b** and 2 cm in **c** and **d**.

In summary, maize and rice *SWEET4* genes encode hexose transporters likely acting downstream of a cell wall invertase that hydrolyzes phloem-derived sucrose. ZmSWEET4c and OsSWEET4 appear to be responsible for transferring hexoses across the BETL to sustain development of the large starch-storing endosperm of cereal grains and contribute to sink strength. Reduced sequence variation at *ZmSWEET4c* and *OsSWEET4* intimates that, in both species,

© 2015 Nature America, Inc. All rights reserved.

the respective loci were targets of selection during domestication. Engineering of SWEET hexose transporters may help in generating new high-yield maize and rice varieties. We propose a model for glucose-mediated feed-forward regulation that couples plasma membrane amplification to invertase and SWEET activity. Our work highlights processes analogous to transepithelial sugar import across cells with amplified membrane surface area, mediated by SWEETs in plants and GLUTs in humans. Further work is required to determine whether SWEET4c localizes to both the apical and basal BETL membranes and whether it contributes for both BETL uptake and efflux (**Supplementary Fig. 6**).

URLs. Panzea and HapMap 2, http://www.panzea.org/; Primer3, http://biotools.umassmed.edu/bioapps/primer3_www.cgi; analysis package of libsequence, https://github.com/molpopgen/analysis; msstats, https://github.com/molpopgen/msstats; iPlant data store, directory, iplant/home/shared/panzea/hapmap3/hmp31, in files, c*_hmp31_q30.vcf.gz; Fiji software, http://fiji.sc/Fiji.

METHODS

Methods and any associated references are available in the online version of the paper.

Note: Any Supplementary Information and Source Data files are available in the online version of the paper.

ACKNOWLEDGMENTS

We are grateful to D. Ehrhardt and H. Cartwright for confocal microscopy. For the rice experiments, we are grateful to T. Li for constructing the TALEN vector targeting *OsSWEET4*, B. Liu for rice transgenics, C. Ji for the isolation and transfection of rice protoplasts in the laboratory of B.Y. and X. Li for help with domestication analysis of *OsSWEET4*. We thank M. Greenfield, A. Grimault and K.M. Wong for plant care, Y. Gong for the yeast complementation assay, M. Evans for providing teosinte plant material and C. Stefan for renaming *ZmSWEET4* with "*c*" for her initial. Work performed on maize in the laboratory of W.B.F. was made possible by support from the Office of Basic Energy Sciences of the US Department of Energy under grant DE-FG02-04ER15542, and work on rice was supported by the National Science Foundation under grant IOS-1258018 (B.Y. and W.B.F.); the other laboratories were supported by the National Science Foundation (IOS-1116561 to D.R.M. and K.E.K., IOS-1025976 to K.E.K. and IOS-1238014 to J.R.-I.), as well as USDA-NIFA 2010-04228 (K.E.K., D.R.M. and M.S.).

AUTHOR CONTRIBUTIONS

D.S., P.S.C., P.M.R., J.R.-I., B.Y. and W.B.F. conceived and designed experiments. D.S., D.L., Q.-B.L., J.S., J.Y., G.G., M.S., K.E.K., D.R.M. and J.R.-I. performed experiments. D.S., P.S.C., J.R.-I., B.Y., K.E.K., J.Y., D.R.M. and W.B.F. analyzed the data. D.S. and W.B.F. wrote the manuscript, and J.S., M.S., K.E.K., D.R.M., P.S.C., P.M.R., J.R.-I. and B.Y. revised it.

COMPETING FINANCIAL INTERESTS

The authors declare competing financial interests: details are available in the online version of the paper.

Reprints and permissions information is available online at http://www.nature.com/reprints/index.html.

1. Chourey, P.S., Jain, M., Li, Q.-B. & Carlson, S.J. Genetic control of cell wall invertases in developing endosperm of maize. *Planta* **223**, 159–167 (2006).
2. Wang, E. *et al.* Control of rice grain-filling and yield by a gene with a potential signature of domestication. *Nat. Genet.* **40**, 1370–1374 (2008).
3. Lalonde, S., Wipf, D. & Frommer, W.B. Transport mechanisms for organic forms of carbon and nitrogen between source and sink. *Annu. Rev. Plant Biol.* **55**, 341–372 (2004).
4. Bihmidine, S., Hunter, C.T.I., Johns, C.E., Koch, K.E. & Braun, D.M. Regulation of assimilate import into sink organs: update on molecular drivers of sink strength. *Front. Plant Sci.* **4**, 177 (2013).
5. Glémin, S. & Battaillon, T. A comparative view of the evolution of grasses under domestication. *New Phytol.* **183**, 273–290 (2009).
6. Peng, J. *et al.* 'Green revolution' genes encode mutant gibberellin response modulators. *Nature* **400**, 256–261 (1999).
7. Sekhon, R.S. *et al.* Genome-wide atlas of transcription during maize development. *Plant J.* **66**, 553–563 (2011).
8. Li, G. *et al.* Temporal patterns of gene expression in developing maize endosperm identified through transcriptome sequencing. *Proc. Natl. Acad. Sci. USA* **111**, 7582–7587 (2014).
9. Davidson, R.M., Hansey, C.N. & Gowda, M. Utility of RNA sequencing for analysis of maize reproductive transcriptomes. *Plant Genome* **4**, 191–203 (2011).
10. Hufford, M.B. *et al.* Comparative population genomics of maize domestication and improvement. *Nat. Genet.* **44**, 808–811 (2012).
11. Chen, L.-Q. *et al.* Sugar transporters for intercellular exchange and nutrition of pathogens. *Nature* **468**, 527–532 (2010).
12. Chen, L.-Q. *et al.* Sucrose efflux mediated by SWEET proteins as a key step for phloem transport. *Science* **335**, 207–211 (2012).
13. Lin, I.W. *et al.* Nectar secretion requires sucrose phosphate synthases and the sugar transporter SWEET9. *Nature* **508**, 546–549 (2014).
14. Lemmon, Z.H. *et al.* The role of *cis* regulatory evolution in maize domestication. *PLoS Genet.* **10**, e1004745 (2014).
15. Chourey, P.S., Li, Q.-B. & Cevallos-Cevallos, J. Pleiotropy and its dissection through a metabolic gene *Miniature1* (*Mn1*) that encodes a cell wall invertase in developing seeds of maize. *Plant Sci.* **184**, 45–53 (2012).
16. Flint-Garcia, S.A., Bodnar, A. & Scott, M.P. Wide variability in seed characteristics, kernel quality, and zein profiles among diverse maize inbreds, landraces, and teosinte. *Theor. Appl. Genet.* **119**, 1129–1142 (2009).
17. Sosso, D., Javelle, M. & Rogowsky, P.M. in *Advances in Maize* Vol. 3 (eds. Prioul, J.L., Thevenot, C. & Molnar, T.) 163–188 (Society for Experimental Biology, 2011).
18. Lucas, W.J. *et al.* The plant vascular system: evolution, development and functions. *J. Integr. Plant Biol.* **55**, 294–388 (2013).
19. Chen, L.-Q. *et al.* Embryo nutrition by a cascade of sequentially expressed sucrose transporters in the seed coat. *Plant Cell* **27**, 607–619 (2015).
20. Shannon, J.C. Movement of ^{14}C-labeled assimilates into kernels of *Zea mays* L.: I. pattern and rate of sugar movement. *Plant Physiol.* **49**, 198–202 (1972).
21. Schmalstig, J.G. & Hitz, W.D. Transport and metabolism of a sucrose analog (1′-fluorosucrose) into *Zea mays* L. endosperm without invertase hydrolysis. *Plant Physiol.* **85**, 902–905 (1987).
22. Cheng, W.H., Taliercio, E.W. & Chourey, P.S. The *Miniature1* seed locus of maize encodes a cell wall invertase required for normal development of endosperm and maternal cells in the pedicel. *Plant Cell* **8**, 971–983 (1996).
23. Koch, K. Sucrose metabolism: regulatory mechanisms and pivotal roles in sugar sensing and plant development. *Curr. Opin. Plant Biol.* **7**, 235–246 (2004).
24. Xiong, Y., Li, Q.-B., Kang, B.-H. & Chourey, P.S. Discovery of genes expressed in basal endosperm transfer cells in maize using 454 transcriptome sequencing. *Plant Mol. Biol. Rep.* **29**, 835–847 (2011).
25. Klemens, P.A.W. *et al.* Overexpression of the vacuolar sugar carrier AtSWEET16 modifies germination, growth, and stress tolerance in *Arabidopsis*. *Plant Physiol.* **163**, 1338–1352 (2013).
26. Guo, W.J. *et al.* SWEET17, a facilitative transporter, mediates fructose transport across the tonoplast of *Arabidopsis* roots and leaves. *Plant Physiol.* **164**, 777–789 (2014).
27. Tao, Y. *et al.* Structure of a eukaryotic SWEET transporter in a homotrimeric complex. *Nature* doi:10.1038/nature15391 (19 October 2015).
28. Chen, H.-Y. *et al.* The *Arabidopsis* vacuolar sugar transporter SWEET2 limits carbon sequestration from roots and restricts *Pythium* infection. *Plant J.* **83**, 1046–1058 (2015).
29. Wieczorke, R. *et al.* Concurrent knock-out of at least 20 transporter genes is required to block uptake of hexoses in *Saccharomyces cerevisiae*. *FEBS Lett.* **464**, 123–128 (1999).
30. Kellett, G.L., Brot-Laroche, E., Mace, O.J. & Leturque, A. Sugar absorption in the intestine: the role of GLUT2. *Annu. Rev. Nutr.* **28**, 35–54 (2008).
31. Zheng, Y. & Wang, Z. Current opinions on endosperm transfer cells in maize. *Plant Cell Rep.* **29**, 935–942 (2010).
32. Thompson, R.D., Hueros, G., Becker, H.A. & Maitz, M. Development and functions of seed transfer cells. *Plant Sci.* **160**, 775–783 (2001).
33. Wardini, T., Talbot, M.J., Offler, C.E. & Patrick, J.W. Role of sugars in regulating transfer cell development in cotyledons of developing *Vicia faba* seeds. *Protoplasma* **230**, 75–88 (2007).
34. Gómez, E. *et al.* The maize transcription factor Myb-related protein-1 is a key regulator of the differentiation of transfer cells. *Plant Cell* **21**, 2022–2035 (2009).
35. Barrero, C. *et al.* The promoter of ZmMRP-1, a maize transfer cell–specific transcriptional activator, is induced at solute exchange surfaces and responds to transport demands. *Planta* **229**, 235–247 (2009).
36. Borisjuk, L. *et al.* Seed development and differentiation: a role for metabolic regulation. *Plant Biol.* **6**, 375–386 (2004).
37. Eom, J.S. *et al.* SWEETs, transporters for intracellular and intercellular sugar translocation. *Curr. Opin. Plant Biol.* **25**, 53–62 (2015).
38. Huang, X. *et al.* A map of rice genome variation reveals the origin of cultivated rice. *Nature* **490**, 497–501 (2012).

© 2015 Nature America, Inc. All rights reserved.

ONLINE METHODS

Maize plant material and growth conditions. The *zmsweet4c-umu1* and *zmsweet4c-umu2* alleles were obtained from the UniformMu transposon population[39]: *zmsweet4c-umu1* (UFMu-07993) from the Maize Genetics Cooperation Stock Center and *zmsweet4c-umu2* by Mu-seq profiling[40,41] of seed mutants from the population. Allelism of *zmsweet4c-umu1* and *zmsweet4c-umu2* was confirmed by genetic complementation tests with reciprocal crosses between heterozygous plants. The *zmsweet4c-umu1* mutation was propagated as a heterozygote by transmission through the female and selection for *emp* kernels. Homozygous seeds were germinated on sterile filter paper with sterile water 3 d in the dark at 30 °C. Wild-type or heterozygous plants were grown side by side for each experiment, either in summer field conditions (Stanford Campus, California, USA) or in greenhouses under long-day conditions (16-h day/8-h night). To further characterize *emp* mutants, sagittal sections of seed at 15 DAP were cut with a utility knife. Seed weight was assessed on seed isolated form segregating ears grown in the summer field. Ten seeds were weighed together on a laboratory scale (Sartorius Extend), in three pools of ten seeds per ear for a total of ten ears.

Maize and teosinte sequencing. A small panel of five maize inbred lines (A188, A619, B73, Mo20W and W22) and five *Z. mays* L. ssp. *parviglumis* accessions (Ej15, Ej29, Ms10, S1033 and Collection105) was used to sequence four different regions of *ZmSWEET4c*: (A) −2,146 to −889 bp from the ATG; (B) −1,086 to +22 bp from the ATG; (C1) 0 to +596 bp from the ATG; and (C2) +578 to +1,224 bp from the ATG. Genomic DNA was extracted as described below. The primers to amplify selected sequences are listed in **Supplementary Table 4** and were designed with Primer3. Sequencing was performed by GenScript, and sequences were aligned using SeqMan (DNAStar).

Maize and teosinte sequence analysis. Gene-level nucleotide diversity was downloaded from the maize HapMap 2 Project[42]. Sequence analysis of *ZmSWEET4c* made use of programs in version 0.8.4 of the analysis package of software from the libsequence library[43]. To assess the statistical significance of differentiation between the taxa, we made use of a simple coalescent simulation conditioned on the number of total SNPs observed at each locus that assumes a stable teosinte effective population size of N_e = 150,000. We model domestication as a split between maize and teosinte at 9,000 years before the present[44] with a corresponding maize bottleneck population size of N_b = 2,500 (ref. 45), followed by instant recovery 1,000 years later to an N_e of 150,000. We performed 10,000 coalescent simulations for each locus using a modified version of ms[46], calculating the population differentiation statistic F_{ST} (ref. 47) for each simulation. An example command line for simulation is:

```
ms 7 10000 -s 68 -I 2 2 5 -en 0.013332 0.01667 -ej 0.01521 -eN 0.0151
```

We used vcftools[48] to analyze nucleotide diversity and estimate the frequency of the indel-associated SNP using data from the maize HapMap 3 Project.

Regional association study. A maize diversity panel composed of 282 inbred lines was employed for the regional association study. To conduct the analysis, we obtained genotype-by-sequencing (GBS) data from Panzea and obtained phenotypic data from Flint-Garcia *et al.*[16]. The SNP data were filtered for minor allele frequency (MAF) >0.05 and allele missing rate <50%. After filtering, a total of 306,190 SNPs remained, including 349 SNPs in a 10-Mb region surrounding the *ZmSWEET4c* gene. Association study with the mixed-model method was conducted using the R[1] add-on package GenABEL. First, a kinship matrix was estimated from the genomic data to control for population structure. Second, genome-wide polygenic effects were computed with the polygenic function to control for background quantitative trait loci (QTLs). Finally, the 349 SNPs near the *ZmSWEET4c* gene were tested one by one as the fixed effect and the polygenic QTL effects derived from the previous step were fitted as random effects using the mmscore function.

Genotyping and transcript analysis. Genomic DNA was extracted from maize seedling leaves using BioSprint 96 (Qiagen), according to the supplier's directions. The primer specific to the *ZmSWEET4c* sequence flanking the *Mutator* element was SWT4c-5R, while as transposon-specific primer we used MuINT19. PCR was performed with the Terra PCR Direct Red Dye Premix Protocol (Clontech Laboratories) with a melting temperature of 60 °C. Total RNA was extracted from wild-type maize, teosinte and *zmsweet4c-umu1* seeds collected between 4 p.m. and 6 p.m. using the Spectrum Plant Total RNA kit (Sigma). First-strand cDNA was synthesized using the QuantiTect Reverse Transcription kit following the instructions of the supplier (Qiagen). Primers specific for the last exon and 3′ UTR of *ZmSWEET4c* (ZmSWT4cqF and ZmSWT4cqR) were used for qRT-PCR to determine expression levels using the LightCycler 480 System (Roche). *Zm18s* and *ZmLUG* (amplified using primers Zm18sF and Zm18sR and primers ZmLUGqF and ZmLUGqR, respectively) served as reference genes. The $2^{-\Delta\Delta C_t}$ method was used for relative quantification. All primers are listed in **Supplementary Table 4**.

***In situ* hybridization.** The *ZmSWEET4c* gene was selected for *in situ* hybridization analysis. The gene was cloned using the Zero Blunt TOPO PCR Cloning kit (Invitrogen). The probe was made using 1 µg of total DNA (PCR product from primers M13F and M13R) with SP6 polymerase for the antisense probe and T7 polymerase for the sense probe. The Roche DIG RNA Labeling kit (Roche Diagnostics) was used for the *in vitro* transcription and labeling of antisense and sense RNA probes. *In situ* hybridization was carried out essentially as described[49–51]. Caryopses of the maize inbred accession W22 at 12 DAP were collected, fixed, dehydrated and embedded in Paraplast Plus paraffin (Sherwood Medical Company). A rotary microtome (Microm 325, Carl Zeiss) was used for sectioning of paraffin-embedded caryopses.

FRET sucrose and glucose sensor analysis in HEK293T cells. The *ZmSWEET4c* coding sequence was cloned into the Gateway entry vector pDONR221f1, and the resulting vector was mixed with the destination vector pcDNA3.2V5 for construct expression in HEK293T cells by LR reaction. The analysis was performed as described using two FRET sensors detecting sucrose or glucose[11,52]. Briefly, HEK293T cells were cotransfected with a plasmid carrying the *ZmSWEET4c* coding sequence and the sucrose sensor FLIPsuc90µΔ1V or the glucose sensor FLIPglu600µD13V (100 ng), using Lipofectamine 2000 (Invitrogen) in six-well plates. For FRET imaging, HEK293T/FLIPsuc90µΔ1V cells were perfused with HBSS medium and pulsed with 10 mM sucrose, whereas HEK293T/FLIPglu600µD13V cells were perfused with medium and pulsed with 2.5, 5 or 20 mM glucose. A Leica DM IRE2 inverted fluorescence microscope with a Quant EM camera was used for imaging with SlideBook 4.2 (Intelligent Imaging Innovations) with a 200-ms exposure and an interval of 10 s for sucrose and 15 s for glucose. FRET analyses were performed as described[12]. AtSWEET12 and AtSWEET1 were used as positive controls for sucrose and glucose, respectively, whereas transfection with empty vector served as a negative control. The data shown in **Figure 2c** (this study) and in Figure 3a from Zhou *et al.*[53] are derived from the same day and therefore have the same controls. This was intentional to allow for direct comparison of the data. Experiments have been repeated independently at least three times with comparable results.

EBY4000 growth complementation assay. *ZmSWEET4c* and *OsSWEET4* coding sequences were cloned into the Gateway entry vector pDONR221f1, and the resulting vectors were mixed with destination vector pDRf1-GW for construct expression in yeast by LR reaction. Transformants of the yeast hexose transport mutant EBY4000 (ref. 29) with pDRf1-GW–ZmSWEET4c or pDRf1-GW–OsSWEET4 were first grown on selective synthetic complete (SC) medium (without uracil) containing 2% maltose (Sigma) as the sole carbon source. Drop tests were used to assess the growth of transformed yeast on 2% glucose or fructose solid SD media (OD_{500} = 1, 1:10, 1:100, 1:1,000 and 1:10,000 dilutions; for rice OsSWEET4, 1, 1:10, 1:100 and 1:1,000 dilutions were used). HXT5 yeast served as a positive control, and transformation with empty vector was used as a negative control grown at 30 °C for 4 d. Maltose medium was used as positive growth medium, whereas medium without sugars was used as a negative growth medium. Growth was recorded by scanning the plates on a flatbed scanner.

Plastic embedding and sectioning. Freshly collected maize seeds were placed into a fixative solution of 0.1 M cacodylate buffer with 2% paraformaldehyde and 2% glutaraldehyde, vacuum infiltrated for 15 min and left in the fixative solution overnight. Dehydration followed the fixation step,

© 2015 Nature America, Inc. All rights reserved.

doi:10.1038/ng.3422

with an increasing ethanol gradient (10%, 30%, 50%, 75% and 95%). Plastic embedding was performed accordingly with the LR White embedding kit protocol (Electron Microscopy Science). Semithin cross-sections (1 µm) were cut by Ultracut (Reichert), stained with 0.1% Safranin O for 30 s and then washed twice with distilled water. All sections were mounted with CytoSeal 60 (EM Science).

Endosperm *in vitro* culture and growth conditions. Ears at 5 DAP were sterilized with 95% alcohol followed by immersion for 5 min in 5% bleach under the laminar flow hood. A scalpel was used to remove and longitudinally dissect each grain into two halves. Using a small laboratory scoop, the endosperm was removed from the two halves and placed on plastic Petri dishes with solid medium. The preparation of media was essentially as described[54]: media were supplemented with 1 mg/l of 2,4-dichlorophenoxyacetic acid (2,4-D). All media were adjusted to pH 5.8 before the addition of agar (2.5 g/l) and Phytagel (2 g/l). After autoclaving, streptomycin sulfate (10 mg/l) was filter sterilized into the medium, and 3% glucose, 3% fructose, 3% sucrose, 1.5% glucose + 1.5% fructose, or no sugars were added separately. After 4 d in the dark at 30 °C, endosperms from the same treatments were pooled together, and RNA was extracted from these samples as described above.

Maize seed *in vitro* culture on acarbose medium. Ears at 4 DAP were sterilized with 95% alcohol followed by immersion for 5 min in 5% bleach under the laminar flow hood. A scalpel was used to cut a triangular section with six kernels attached. Blocks with six attached kernels were placed on plastic Petri dishes, each plate with five blocks, containing various media supplemented with sucrose or sucrose + acarbose, and plates were incubated in a dark growth chamber at 28 °C. The preparation of media was essentially as described[54]: media were supplemented with 1 mg/l of 2,4-D. All media were adjusted to pH 5.8 before the addition of agar (2.5 g/l) and Phytagel (2 g/l). After autoclaving, streptomycin sulfate (10 mg/l) was filter sterilized into the medium, and 3% sucrose or 3% sucrose and 50 mM acarbose were added separately. After 5 d, kernels from the same treatment were pooled together, and RNA was extracted from these samples as described above.

Rice plant material, TALEN nuclease mutations and expression profile. The *japonica* rice variety Kitaake was used for TALEN-mediated mutagenesis in *OsSWEET4* (Os02g19820). The methods of TALEN gene synthesis and rice transgenic for production of *ossweet4-1* and *ossweet4-2* were as described[55]. Genes encoding the TALENs recognizing two opposing subsites (left site, TACGGCCTCCCCGCGGTGCACCCGC; right site, TGGCCATGCCGGTGCCGTTGATGGT) in exon 3 of *OsSWEET4* were expressed under the control of the cauliflower mosaic virus (CaMV) *35S* promoter and the maize *Ubiquitin1* promoter, respectively, in rice embryogenic callus cells. Primary transgenic plants with site-specific mutations (4-bp and 7-bp deletions) were self-pollinated, and progeny were selected for homozygous mutation. Plants were grown in either a growth chamber or greenhouse at a temperature of 28–30 °C and relative humidity of 50–75% with a 12-h day/12-h night cycle. Analysis of *OsSWEET4* expression using RT-PCR was performed as described[56].

Transient gene expression of *ZmSWEET4c* in *Nicotiana benthamiana* leaves. The method is described and modified by Bleckmann[57]. The *Agrobacterium tumefaciens* strain GV3101 was transformed with the binary expression clone carrying sequence encoding ZmSWEET4c C-terminally fused with eGFP with expression driven by the constitutive *35S* promoter. Bacterial cultures were grown, precipitated and dissolved in infiltration buffer (10 mM MES, pH 5.6, 10 mM $MgCl_2$ and 200 µM acetosyringone) to a cell density as measured by OD_{600} of approximately 0.5–0.7 for 2 h. A syringe was then used to infiltrate the mixture into the lower surface of *N. benthamiana* leaves. Plants were incubated for 36 to 48 h before imaging. eGFP and chloroplast autofluorescence were detected 3 d after infiltration using a Leica TCS SP5 confocal microscope with simultaneous acquisition at 522–572 nm (eGFP) and 667–773 nm (autofluorescence). Epidermal chloroplasts adhere to the plasma membrane[58] and were therefore used to discriminate whether ZmSWEET4c-eGFP signal was vacuolar (surrounding the chloroplasts) or localized to the plasma membrane (adjacent to the chloroplasts; according to the cell profile in the bright-field image). Image analysis was performed using Fiji software.

Starch quantification. Segregating wild-type and *zmsweet4c-umu1* seeds were collected at 10, 17 and 24 DAP. Seeds were ground to a fine powder with a mortar and pestle in liquid nitrogen, and 50 mg of tissue was incubated with 1 ml of 70% ethanol for 1 h on ice, with frequent vigorous vortexing. Subsequently, the samples were spun for 5 min at 4 °C at 13,000*g*, and the supernatant was removed. This extraction was repeated once. The pellet was subsequently dried in a vacuum concentrator and resuspended in water. Starch was quantified with the Starch Assay kit protocol–UV method (Roche).

Transient gene expression of *OsSWEET4* in rice protoplasts. For the *OsSWEET4:GUS* reporter construct, the promoter fragment 1,102 bp upstream of the translation start site and the terminator region 1,132 bp downstream of the translation stop codon of *OsSWEET4* were PCR amplified, followed by ligation of the β-glucuronidase–coding *uidA* gene between. The whole *OsSWEET4* promoter–*GUS*-terminator cassette was ligated into pCAMBIA1300 at HindIII and EcoRI sites. The mesophyll protoplasts of rice cultivar Kitaake were isolated and transfected using a modified protocol as described[59]. Briefly, the stems and sheaths of seedlings (~5 d old; grown on solid 50% MS medium at 28 °C with a 12-h light/12-h dark cycle) were collected in the morning and cut into small strips, followed by incubation in solution containing 1.5% cellulose RS, 0.75% macerozyme R-10, 0.6 M mannitol, 10 mM MES, 1 mM $CaCl_2$, 5 mM β-mercaptoethanol and 0.1% BSA, pH 5.7, for 6–8 h in the dark with gentle shaking. Released protoplasts were collected and washed with W5 solution (154 mM NaCl, 125 mM $CaCl_2$, 5 mM KCl and 2 mM MES, pH 5.7) before transfection. The reporter construct of *OsSWEET4:GUS* (80 µg) was used to transfect 800 µl (~4×10^6 cells) of protoplasts using a PEG-mediated DNA delivery method. Transfected protoplasts were divided into four parts, each being incubated in medium supplemented with 500 µM mannitol, sucrose, glucose or fructose (in the dark at 28 °C for 12 h) before collection for GUS activity measurement as described[60].

Rice sequence analysis. The *OsSWEET4* region was analyzed for sequence diversity by reanalysis of a haplotype network built from 913 rice accessions within *OsSWEET4* and surrounding regions using fastPHASE36 (ref. 61). Thirteen SNPs in *OsSWEET4* were used to construct the presented haplotype network using a described method[62]. All 305 *indica*-type accessions harbor one haplotype; likewise, the majority of the 204 *japonica* accessions share one haplotype. By contrast, more than ten haplotypes were detected in 387 *Oryza rufipogon* wild rice accessions.

39. McCarty, D.R. *et al.* Steady-state transposon mutagenesis in inbred maize. *Plant J.* **44**, 52–61 (2005).
40. McCarty, D.R. *et al.* Mu-seq: sequence-based mapping and identification of transposon induced mutations. *PLoS ONE* **8**, e77172 (2013).
41. Hunter, C.T. *et al.* Phenotype to genotype using forward-genetic Mu-seq for identification and functional classification of maize mutants. *Front. Plant Sci.* **4**, 545 (2014).
42. Hufford, M.B. *et al.* Comparative population genomics of maize domestication and improvement. *Nat. Genet.* **44**, 808–811 (2012).
43. Thornton, K. *et al.* Libsequence: a C. class library for evolutionary genetic analysis. *Bioinformatics* **19**, 2325–2327 (2003).
44. Piperno, D.R. *et al.* Starch grain and phytolith evidence for early ninth millennium B.P. maize from the Central Balsas River Valley, Mexico. *Proc. Natl. Acad. Sci. USA* **106**, 5019–5024 (2009).
45. Wright, S.I. *et al.* The effects of artificial selection on the maize genome. *Science* **308**, 1310–1314 (2005).
46. Hudson, R.R. *et al.* Generating samples under a Wright-Fisher neutral model of genetic variation. *Bioinformatics* **18**, 337–338 (2002).
47. Hudson, R.R. *et al.* A statistical test for detecting geographic subdivision. *Mol. Biol. Evol.* **9**, 138–151 (1992).
48. Danecek, P. *et al.* The variant call format and VCFtools. *Bioinformatics* **27**, 2156–2158 (2011).
49. Jackson, D.P. in *Molecular Plant Pathology: A Practical Approach* (eds. Bowles, D.J., Gurr, S.J. & McPhereson, M.) 163–174 (Oxford University Press, 1991).
50. Wang, C. *et al.* Isolation and characterization of expressed sequence tags (ESTs) from cambium tissue of birch (*Betula platyphylla* Suk). *Plant Mol. Biol. Rep.* **28**, 438–449 (2010).
51. De Oliveira, R.R. *et al. In silico* and quantitative analyses of MADS-Box genes in *Coffea arabica*. *Plant Mol. Biol. Rep.* **28**, 460–472 (2010).
52. Hou, B.H. *et al.* Optical sensors for monitoring dynamic changes of metabolite levels in mammalian cells. *Nat. Protoc.* **6**, 1818–1833 (2011).
53. Zhou, J. *et al.* Gene targeting by the TAL effector PthXo2 reveals cryptic resistance gene for bacterial blight of rice. *Plant J.* **82**, 632–643 (2015).

© 2015 Nature America, Inc. All rights reserved.

54. Cheng, W.H. & Chourey, P.S. Genetic evidence that invertase-mediated release of hexoses is critical for appropriate carbon partitioning and normal seed development in maize. *Theor. Appl. Genet.* **98**, 485–495 (1999).
55. Li, T. *et al.* TALEN utilization in rice genome modifications. *Methods* **69**, 9–16 (2014).
56. Li, T. *et al.* High efficiency TALEN-based gene editing produces disease resistant rice. *Nat. Biotechnol.* **30**, 390–392 (2012).
57. Bleckmann, A. *et al.* Stem cell signaling in *Arabidopsis* requires CRN to localize CLV2 to the plasma membrane. *Plant Physiol.* **152**, 166–176 (2010).
58. Dupreet, P. *et al.* Expression of photosynthesis gene-promoter fusions in leaf epidermal cells of transgenic tobacco plants. *Plant J.* **1**, 115–120 (1991).
59. Zhang, Y. *et al.* A highly efficient rice green tissue protoplast system for transient gene expression and studying light/chloroplast-related processes. *Plant Methods* **7**, 30 (2011).
60. Jefferson, R.A., Kavanagh, T.A. & Bevan, M.W. GUS fusions: β-glucuronidase as a sensitive and versatile gene fusion marker in higher plants. *EMBO J.* **6**, 3901–3907 (1987).
61. Scheet, P. & Stephens, M. A fast and flexible statistical model for large-scale population genotype data: applications to inferring missing genotypes and haplotypic phase. *Am. J. Hum. Genet.* **78**, 629–644 (2006).
62. Paradis, E. pegas: an R package for population genetics with an integrated-modular approach. *Bioinformatics* **26**, 419–420 (2010).

© 2015 Nature America, Inc. All rights reserved.